Millions of Boreal Shield Lakes can be used to Probe the Evolution of Archaean Ocean Life

Schiff SL[1], Tsuji JM[1], Wu L[1], Venkiteswaran JJ[1,2], Molot L[3], Elgood RJ[1], Paterson MJ[4], and JD Neufeld[1]

[1]University of Waterloo, 200 University Ave W, Waterloo, Ontario, N2L 3G1, Canada (sschiff@uwaterloo.ca, jneufeld@uwaterloo.ca)

[2]Wilfrid Laurier University, 75 University Ave W, Waterloo Ontario, N2L 3C5, Canada

[3]York University, 4700 Keele Street, Toronto, Ontario, M3J 1P3, Canada

[4]IISD-Experimental Lakes Area, 111 Lombard Ave Suite 325, Winnipeg MB R3B 0T4, Canada

Abstract

Ancient oceans on Earth were rich in iron, low in sulfur, and free of oxygen. The evolution of life, the onset of photosynthesis, and the subsequent oxidation of Earth's early oceans and atmosphere have long fostered intense debate. Very few analogous modern systems have been identified for study and most evidence has been gleaned from the sedimentary rock record, spurred by controversy surrounding the origin of the globally ubiquitous and extensive banded iron formations (BIFs). Here we provide the first evidence that Boreal Shield lakes can serve as modern analogues for the Archaean ocean. Specifically, we combine isotopic and molecular data to demonstrate that photoferrotrophy, a process involving photosynthetic fixation of carbon using reduced iron as an electron donor, occurs in the anoxic zone of stratified boreal lakes that are naturally low in sulfur and rich in iron. Further, anoxygenic photosynthetic processes are active in the water column, are prominent in the total metabolism of these bottom waters, and are marked by distinctive patterns in naturally occurring isotopes of carbon, nitrogen, and iron. Most importantly, these processes are robust, returning after water column re-oxygenation following lake turnover. Evidence of coupled iron oxidation, iron reduction, and methane oxidation has implications for both early Earth and modern systems. Previous studies have been confined to permanently stratified but low sulfur lakes on the assumption that photoferrotrophic bacteria are oxygen intolerant. Given that Boreal Shield lakes and ponds number in the tens of millions, and several can be manipulated experimentally, opportunities for exploring the evolution of life on ancient Earth are now greatly expanded.

Almost one half of the largest terrestrial biome on Earth, the boreal forest, is underlain by Precambrian Shield geology[1] of low sulfur content. Lakes cover over 7% of the Boreal Shield areas of Canada, Fennoscandinavia, and Russia[2]. If the supply of terrestrial or aquatic organic matter is sufficient and/or the lake morphometry restricts mixing, bottom portions of stratified lakes and shallow ponds can become anoxic periodically in summer and under ice in winter. Low sulfur and anoxic conditions result in high Fe concentrations. Thus environmental conditions in these waters are comparable to the early Archaean ocean[3].

Bacterial photosynthesis is important in modern systems but key to the early evolution of life and atmospheric oxygen on Earth. Only a few modern analogues of the Archaean ocean have been identified[3]. In a pioneering study in Lake Matano, Indonesia, a significant population of photosynthetic green sulfur bacteria (GSB) were found just below the permanent chemocline at 120 metres depth, including an organism similar to *Chlorobium ferrooxidans*, a known photoferrotroph[4]. This organism uses light to fix inorganic carbon to organic carbon with reduced iron (Fe^{2+}) as the electron donor, thereby producing oxidized iron:

$$4\ Fe^{2+} + HCO_3^- + 10\ H_2O \xrightarrow{hv} CH_2O + 4\ Fe(OH)_3 + 7\ H^+$$

Photoferrotrophy has been proposed as the earliest photosynthetic process in Earth's history, predating oxygenic photosynthesis by cyanobacteria[5]. Photoferrotrophy could be responsible for a large part of early Earth oxidation leading to the mixed Fe oxidation states that have proven difficult to explain in globally occurring BIFs, deposited when oxygen was still absent from the atmosphere[5,6]. Since the initial discovery at Lake Matano, only two other open water sites (Lac Cruz, Spain[3]; subbasin of Lake Kivu[7], east Africa) have been identified that host possible photoferrotrophs within the GSB (phylum *Chlorobi*). Very recently, the first metabolic rate measurements have been reported in the chemoclines of Lakes Kivu and Cruz, confirming photoferrotrophic activity and its biogeochemical importance by fueling microbial iron reduction

and possibly co-existing pelagic heterotrophy. No other examples of microbial consortia have yet been reported in conditions that mimic the Archaean ocean. All of these systems are meromictic and have low sulfate and high iron due to their origins as volcanic craters or rift lakes. Such systems are naturally rare worldwide[7], with expectations that only a handful of appropriate lakes will be found[8]. This limits progress toward understanding Archaean ocean biogeochemistry and the origins of life.

Boreal Shield lakes have been intensely studied at the Experimental Lakes Area (ELA) in northwestern Ontario, Canada. One of these small lakes, Lake 227 (L227), is the site of the world's longest running nutrient addition experiment, with varying additions of nitrogen and phosphorus or phosphorus alone for over 47 years[9]. Summer phytoplankton biomass is high, resulting in a hypolimnion that is devoid of oxygen. However, the presence of over 50 cm of continuous annually varved sediments in the deepest part of the lake (10 m)[10] indicates that the bottom of the hypolimnion has been naturally anoxic during lake stratification for over 300 years. Nearby Lake 442 (L442) has not been manipulated experimentally and is typical of natural lakes on the Boreal Shield.

Hypolimnetic waters in L227 have distinctive patterns in natural abundance stable isotopes (Fig. 1). These waters are high in iron, ammonium (NH_4^+), dissolved inorganic carbon (DIC), and methane (CH_4) and low in sulfate (Supplementary Data Fig. 1). Stable carbon isotopes ($\delta^{13}C$) of particulate organic matter (POM) in the hypolimnion were offset from the overlying epilimnion where phytoplankton biomass was high. In contrast, hypolimnetic sediments and sediment trap samples were similar in $\delta^{13}C$ to epilimnetic POM, consistent with the high flux of organic carbon from the surface and indicating that the offset in $\delta^{13}C$ was not an effect of POM diagenesis during transit through the short water column to lake sediments.

Further, $\delta^{13}C$ of hypolimnetic DIC increased with depth. Hypolimnetic POM of lower $\delta^{13}C$ than either epilimnetic POC or hypolimnetic DIC can only be attributed to isotopic fractionation associated with photosynthesis or assimilation of C with very negative $\delta^{13}C$, such as that measured in CH_4. Similarly, nitrogen isotopic composition ($\delta^{15}N$) of hypolimnetic POM was offset from epilimnetic POM and hypolimnetic NH_4^+, consistent with isotopic fractionation during biological uptake. Finally, the $\delta^{56}Fe$ of POM in the epilimnion and hypolimnion also differed and the isotopic fractionation between dissolved and particulate phase was reversed from the epilimnion to hypolimnion. Rates of vertical mixing in the hypolimnion previously determined using additions of ^{226}Ra and ^{3}H as tracers are very low[11,12], similar to rates of molecular diffusion. Low mixing rates imply that microbiota contributing to hypolimnetic POM are suspended in the water column at that depth, are metabolically active and sufficiently abundant to alter the isotopic POM signatures of $\delta^{13}C$, $\delta^{15}N$, and $\delta^{56}Fe$ in POM from values typical of the epilimnion. Furthermore, the offset of the stable isotopes in POM from inorganic dissolved substrates is consistent with fractionation associated with photosynthesis, even though light levels in the hypolimnion are extremely low due to high summer epilimnetic biomass.

Throughout the L227 hypolimnion, we detected abundant iron-cycling bacteria, along with a community of sulfur and methane cyclers, a microbial consortium similar to that in Lake Kivu, where photoferrotrophic activity was found[13]. High-throughput sequencing of bacterial 16S ribosomal RNA (16S rRNA) genes from L227 water column samples (Fig. 2) showed *Chlorobi*, closely related to *C. ferrooxidans*, among the most abundant operational taxonomic units (OTUs) in the anoxic zone. Sequences classified within the genus *Chlorobium* comprised up to 8% of all reads just below the oxic-anoxic interface. One particular *Chlorobium* OTU (Fig. 2, *Chlorobium* sp. 1), which was the most abundant across all L227 samples, had over 99.5% 16S rRNA gene

110 sequence identity with known *C. ferrooxidans* strains (Supplementary Data Fig. 2). Based on 16S rRNA gene functional inferences, the hypolimnion of L227 also supports a metabolically unique bacterial community. The hypoxic and anoxic zones of L227 were rich in bacterial iron reducers, including members of the genera *Rhodoferax*, *Geothrix*, and *Aldibiferax*. These taxa were abundant just above and where *Chlorobi* were identified, potentially reducing Fe(III) produced
115 by photoferrotrophic activity and chemical oxidation. Abundant methanotrophic OTUs belonging to the family *Methylococcaceae* were also detected. In contrast, potential S-oxidizers and reducers, such as *Sulfuritalea* and *Desulfatirhabdium* spp., were lower in abundance, implying relatively low contributions to overall lake metabolism. Such distinctive pelagic microbial consortia of Fe oxdizers, Fe reducers, and methanotrophs have not been reported outside of
120 the few modern analogues of the Archaean ocean.

Key evidence of photoferrotrophy is provided by stable iron isotopes, a tool only very recently applied to freshwater lake iron cycling[13,14], and not yet in Lakes Matano or Kivu. In the anoxic hypolimnion of L227, δ^{56}Fe in suspended particulates does not match any other particulate or dissolved pool in the water column or sediments (Fig. 1c). Further, observed differences in
125 δ^{56}Fe between dissolved and particulate Fe are consistent in magnitude and direction with that of other ferrotrophs in laboratory cultures[15]. Although we cannot rule out the possibility of isotopic separation due to partial iron oxidation at the oxycline, the high population of iron-reducing bacteria in the metalimnion and hypolimnion implies that most or all accessible and re-oxidized iron should be reduced rapidly. This allows the hypolimnetic iron isotope signatures to be
130 interpreted as the result of biological rather than chemical processes. The similarity of δ^{56}Fe in the hypolimnetic dissolved phase, epilimnetic POM and sediments, and the offset between hypolimnetic and epilimnetic POM (concomitant with δ^{13}C and δ^{15}N evidence), indicate that the

δ^{56}Fe signature in hypolimnetic POM results from microorganisms residing at that depth. Together, our data indicate that iron isotopes are diagnostic of photoferrotropic activity in softwater lakes.

Photoferrotrophy is not confined to experimentally eutrophied L227. Similar geochemistry and microbiota were identified in unperturbed L442. Lake 442 has both an anoxic zone and overlying oxic portion within the hypolimnion. In the anoxic hypolimnion, δ^{13}C, δ^{15}N, and water column chemistry (high Fe, DIC and NH_4^+, and low SO_4^{2-}) are typical of anoxic hypolimnia in other ELA lakes. Patterns in particulate and dissolved phase δ^{13}C, δ^{15}N, and δ^{56}Fe in L442 are all consistent with the anoxic hypolimnion of L227, and distinctly different from the oxic hypolimnion (Fig. 1). Molecular sequencing in the anoxic zone confirmed high abundance of *Chlorobi* that are closely related to *C. ferrooxidans*, in addition to a similar microbial consortium of putative iron reducers, sulfur reducers and oxidizers, and methanotrophs (Fig. 2). Thus, these Archaean ocean analogue processes likely occur in Boreal Shield lakes with seasonally anoxic hypolimnia because the geology naturally leads to low sulfate and high iron conditions. Observations of both *Chlorobi* and methanotrophs have been reported in anoxic hypolimnia in numerous Boreal Shield lakes in Finland[16,17,18], added support that these processes are widespread. Here we present first evidence of photoferrotrophy in Boreal Shield lakes, demonstrate that these globally abundant systems can be used as Archaean ocean analogues, and show how easily recognized patterns of isotopic, chemical, and molecular indicators can be used to prospect for these distinctive microbial consortia.

Important and novel to the debate surrounding evolution of life in the Archaean ocean is that the microbial consortia associated with photoferrotrophy are robust and establish rapidly. Both L227 and L442 have two mixing periods per year with fall turnover being the most

complete. In wind protected L227, the water column is well oxygenated to at least 6 m every year in both spring and fall where *Chlorobium* spp. are abundant (Fig. 3 and Supplementary Data Fig. 3). In L442, mixing is complete in both spring and fall (Supplementary Data Fig. 4). Geochemical, isotopic, and molecular analyses over several years show that these characteristic microbial consortia are re-established following oxygenation (Fig. 2). Although *Chlorobi* and methanotrophs have been found to re-establish in other lake hypolimnia following turnover[17,19], our study is the first to show that the microbial consortia associated with photoferrotrophy are resilient.

Exploring the physicochemical conditions and isotopic fractionations associated with these microbial consortia will spur advances in understanding of both modern and ancient systems. A strain of the filamentous cyanobacterium *Aphanizomenon schindlerii* was also observed at 6.5 m[20], leaving open the possibility that a hypothesized precursor to oxygenic photosynthesis may still be operating today under similar conditions to early anoxic oceans. We report first evidence of distinctive microbial fractionation in iron isotopes *in situ* in an Archaean analogue setting. Probing conditions in modern systems will facilitate new interpretations of the wide range of iron isotopic values observed in BIFs. Similarly, our carbon isotope results have implications for both modern and ancient carbon cycling. Consumption of dissolved CH_4 with very low $\delta^{13}C$, perhaps by abundant methanotrophs in the anoxic zone, must contribute to L227 POM to offset the high flux of transitory organic matter and associated heterotrophic activity with much higher $\delta^{13}C$. Isotopic fractionation inherent in the reductive citric acid pathway, hypothesized as the photosynthetic pathway for GSB[5,7] is too small. Use of CH_4 as a carbon substrate within such microbial consortia could alter interpretation of the $\delta^{13}C$ signature for photosynthesis in ancient rocks and in modern settings, such as Lake Kivu[7]. Biogenic CH_4 is

hypothesized to be an important contributor to the Archaean atmosphere[21]. Anaerobic
180 consumption of biogenic CH_4 also has implications for carbon cycling and oxidation in ancient oceans. In addition, analyses of $\delta^{15}N$ show evidence of isotopic fractionation when large amounts of NH_4^+ are present. Little is known about N cycling in the Archaean ocean or whether this isotopic signal is preserved in the geologic record.

Our finding of active microbial iron oxidation in anoxic hypolimnia of boreal shield lakes
185 also has novel implications for limnology, water management and microbial ecology. The overall importance of internal iron reduction-oxidation to metabolism within the anoxic hypolimnetic water column, including the presence of a putative iron oxidizer and high relative abundance and diversity of iron reducers, has not yet been recognized. Metabolism of methanotrophs that are present in high abundance in the anoxic zone has been suggested to be coupled to oxygen
190 produced by cyanobacteria at the same depth[22], but it is also possible that this process may be coupled with reduction of newly oxidized iron by photoferrotrophs. Metagenomic data may shed light on these processes that have been identified in other anoxic and low S aquatic habitats[23,24]. The importance of methanotrophy in anoxic hypolimnia with respect to either metabolism or CH_4 emissions to the atmosphere is only starting to receive scrutiny[19,22], and not
195 yet in the context of the metabolic pathways of the entire microbial consortium. Further, availability of reduced iron has recently been implicated as a factor controlling dominance of cyanobacteria in both non-eutrophic systems and in recent increases in formation of hazardous algal blooms[20]; further understanding of iron redox cycling is urgently needed. Also unknown is the role of oxidized iron production in anoxic hypolimnia with respect to sequestration of
200 phosphorous, the limiting nutrient in most boreal shield lakes. L227 and similar boreal lakes have atypical low internal phosphorous release[25]. Lastly, some iron cycling organisms are known to

play a role in mercury (Hg) cycling and formation of methylated Hg[26], a toxic and bioaccumulating contaminant of fish in Boreal Shield lakes.

Using real systems is a powerful approach for promoting new discoveries. In contrast to simplified and hard to maintain laboratory cultures, whole microbial communities can be studied under *in situ* environmental conditions. Boreal lakes and ponds number in the tens of millions[27] and, of these, some 15% could have a portion of the water column that is seasonally anoxic, opening new avenues of exploration. Water column chemistry and light penetration differ considerably among boreal lakes depending on geology and contribution of dissolved organic carbon from the catchment. Thus, broad gradients of physico-chemical conditions such as flux and quality of organic matter, sulfate and sulfide concentrations and light penetration can be exploited to better understand these unique microbial communities. Furthermore, small lakes, such as those at ELA, can also be manipulated experimentally so that a specific range of conditions can be targeted or purposeful additions of carbon or iron isotope tracers can be used to probe isotopic fractionation *in situ*. Because hypolimnia become isolated during the stratified period, mass balances can be used to infer metabolic pathways, products, and rates. Coupling these data to parallel metagenomic and metatranscriptomic analyses will facilitate reconstruction of genomes and active metabolic processes associated with observed photoferrotrophy. In addition, isotopic fractionations of $\delta^{13}C$, $\delta^{15}N$, and $\delta^{56}Fe$ associated with anoxygenic photosynthesis and iron cycling that may be preserved in the global rock record can be studied *in situ* and during early stages of diagenesis in lake sediments deposited over the last 10,000 years since deglaciation. Boreal Shield lakes provide natural and accessible incubators for the study of the evolution of life in early Earth history.

Acknowledgements We thank researchers at the Experimental Lakes Area who amassed an unparalleled dataset over the past 46 years providing crucial data for shorter term studies. We thank D.W. Schindler, R.E. Hecky, W.D. Taylor, and C. Welte for critical reading of the manuscript; S. McCabe and staff at the Experimental Lakes Area for technical help with chemical analyses; K. Liu for δ^{56}Fe analysis, C. Johnson and B. Beard for providing the facility for δ^{56}Fe analysis, and K. Engel for assistance with sequencing. All authors were funded by the National Sciences and Engineering Research Council of Canada (NSERC) and the Water Institute at the University of Waterloo, Canada.

References

1. Venkiteswaran J. J., Schiff, S. L. & Wallin, M. B. Large carbon dioxide fluxes from headwater boreal and sub-boreal streams. *PLoS ONE* **9** (2014).

2. Kortelainen, P., Pajunen, H., Rantakari, M. & Saarnisto, M. A large carbon pool and small sink in boreal Holocene lake sediments. *Global Change Biol*, **10,** 1648–1653 (2004).

3. Walter, X. A. *et al*. Phototrophic Fe (II)-oxidation in the chemocline of a ferruginous meromictic lake. *Front. Microbiol.* **5,** 713 (2014).

4. Crowe, S. A. *et al*. Photoferrotrophs thrive in an Archean Ocean analogue. *Proc. Natl. Acad. Sci. USA* **105,** 15938-15943 (2008).

5. Konhauser, K. O. Introduction to Geomicrobiology. Blackwell Publishing, Malden, MA, USA. 440pp. (2006).

6. Kappler, A., Pasquero, C., Konhauser, K. O. & Newman, D. K. Deposition of banded iron formations by anoxygenic phototrophic Fe(II)-oxidizing bacteria. *Geology* **33,** 865-868 (2005).

7. Llirós, M. *et al*. Pelagic photoferrotrophy and iron cycling in a modern ferruginous basin. *Sci. Rep.* **5**, 13803 (2015).

8. Koeksoy, E., Halama, M., Konhauser, K. O. & Kappler, A. Using modern ferruginous habitats to interpret Precambrian banded iron formation deposition. *Intl. J. Astrobiol*. doi:10.1017/S1473550415000373 (2015).

9. Schindler, D. W. *et al*. Eutrophication of lakes cannot be controlled by reducing nitrogen input: results of a 37-year whole-ecosystem experiment. *Proc. Natl. Acad. Sci. USA* **105,** 11254–11258 (2008).

10. Wolfe, B., Kling H. J., Brunskill G. J., & Wilkinson, P. Multiple dating of a freeze core from Lake 227, an experimentally fertilized lake with varved sediments. *Can. J. Fish. Aquat. Sci*. **51,** 2274-2285 (1994).

11. Emerson, S. R. & Hesslein, R. H. Distribution and uptake of artificially introduced radium-226 in a small lake. *J. Fish. Res. Board Can*. **30**, 1485-1490 (1973).

12. Quay, P. D., Broecker, W. S., Hesslein, R. H. & Schindler, D. W. Vertical diffusion rates determined by tritium tracer experiments in the thermocline and hypolimnion of two lakes. *Limnol. Oceanogr.* **25**, 201-218 (1980).

13. Busigny, V. *et al*. Iron isotopes in an Archean ocean analogue. *Geochim. Cosmochim. Acta* **133,** 443-462 (2014).

14. Liu, K., Wu, L., Couture, R.-M., Li, W. & Van Cappellen, P. Iron isotope fractionation in sediments of an oligotrophic freshwater lake. *Earth Planet. Sci. Lett.* **423**, 164-172 (2015).

15. Croal, L. R., Johnson, C. M., Beard, B. L. & Newman, D. K. Iron isotope fractionation by Fe(II)-oxidizing photoautotrophic bacteria. *Geochim. Cosmochim. Acta* **68,** 1227-1242 (2004).

16. Karhunen, J., Arvola, L., Peura, S. & Tiirola, M. Green sulphur bacteria as a component of the photosynthetic plankton community in small dimictic humic lakes with an anoxic hypolimnion. *Aquat Microb Ecol* **68**, 267–272 (2013).

17. Hanson, T. E., Luther, G. W. I., Findlay, A., MacDonald, D. & Hess, D. Phototrophic sulfide oxidation: environmental insights and a method for kinetic analysis. *Front. Microbiol.* **4**, 382 (2013).

18. Taipale, S., Kankaala, P., Hahn, M. W., Jones, R. I. & Tiirola, M. Methane-oxidizing and photoautotrophic bacteria are major producers in a humic lake with a large anoxic hypolimnion. *Aquat. Microb. Ecol.* **64**: 81–95 (2011).

19. Oswald, K. *et al*. Light-Dependent Aerobic Methane Oxidation Reduces Methane Emissions from Seasonally Stratified Lakes. *PLoS ONE* **10**(7) (2015).

20. Molot, L. A. *et al*. A novel model for cyanobacteria bloom formation: The critical role of anoxia and ferrous iron. *Freshwater Biol.* **59,** 1323-1340 (2014).

21. Zerkle, A. L., Claire, M. W., Domagal-Goldman, S. D., Farquhar, J. & Poulton, S. W. A bistable organic-rich atmosphere on the Neoarchaean Earth, *Nat. Geosci.* **5**, 359-363 (2012).

22. Milucka, J. *et al*. Methane oxidation coupled to oxygenic photosynthesis in anoxic waters. *ISME* **9**, 1991–2002 (2015).

23. Beal, E. J., Claire, M. W. & House, C. H. High rates of anaerobic methanotrophy at low sulfate concentrations with implications for past and present methane levels. *Geobiology* **9**, 131-139 (2011).

24. Scheller, S., Yu, H., Chadwick, G. L. , McGlynn, S. E. & Orphan, V. J. Artificial electron acceptors decouple archaeal methane oxidation from sulfate reduction. *Science*. **351**, 703-707 (2016).

25. Findlay, D. L. & Kasian S. E. M. Phytoplankton community responses to nutrient addition in Lake 226, Experimental Lakes Area, northwestern Ontario. *Can. J. Fish. Aquat. Sci.* **44 (Suppl. 1)**, 35-46 (1987).

26. Grégoire, D. S. & Poulain, A. J. A physiological role for Hg^{II} during phototrophic growth. *Nat. Geosci*. **9**, 121-125 (2016).

27. Verpoorter, C., Kutser, T., Seekell, D. A. & Tranvik, L. J. A global inventory of lakes based on high-resolution satellite imagery. *Geophy. Res. Lett.* **41**, 6396-6402 (2014).

Methods

Site description

The Experimental Lakes Area (ELA) is located in northwestern Ontario, Canada at 49°40' N, 93°45' W. Information on geology, vegetation and climate is available[28]. Lake 227 is a small headwater lake of 5 ha with a mean depth of 4.4 meters and maximum depth of 10 m. Lake 442 is a small lake of 16 ha with a mean depth of 9.6 meters and maximum depth of 17.8 m.

Sample collection and analysis

Water and lake sediment samples from Lake 227 have been collected from the beginning of the nutrient addition experiment in 1969 and continue today. For this study, water, sediment trap and sediment samples were collected over several years. Multiple water column profiles were collected in Lake 227 in 2010 and 2011 during the summer stratified period from May to October. Single profiles were collected around the time of the cyanobacterial bloom that occurs each year in June to July in 2012, 2013 and 2014. The most complete data for all parameters is given in the figures with dates of sampling.

Water samples were collected using a peristaltic pump in a closed system from the desired depth. Samples for NO_3^-, NH_4^+, DOC, SO_4^{2-}, and total dissolved Fe (TDFe) were filtered shortly after collection with 0.45 μm filters and analyzed using conventional methods[29]. Sulfide was measured with an ion selective electrode (ISE) on unfiltered samples following stabilization in a sulfide anti-oxidant buffer[30]. However, it is recognized that "free sulfide" is overestimated by an order of magnitude using the commonly used methylene blue method for dissolved samples due to the presence of "multiple reduced diffusible sulfur species"[4]. The contribution of dissolved, colloidal and particulate sulfur species to the response by the ISE in our unfiltered samples is unknown but most likely causes a substantial overestimation of "free sulfide" species. NO_3^- is very low in both the epilimnion and hypolimnion for these lakes with mean values of < 3.2 μM in the summer

stratified period. Water column light levels are routinely measured at ELA in the ice-free seasons using a LICOR flat plate quantum sensor (LI-192). As a result of light scattering and absorption associated with high phytoplankton densities in L227, PAR is strongly attenuated over depth and only a very small proportion of surface irradiance reaches the hypolimnion. Throughout the May-Oct period, PAR values at 6 m depth in L227 were <1.5 $\mu E \bullet m^{-2} \bullet sec^{-1}$.

Samples for concentrations and isotopic analysis of DIC and CH_4 were collected directly without headspace into small glass serum bottles with stoppers and preserved with injections of concentrated HCl. Particulate organic matter (POM) for isotopic analysis was collected on Whatman QMA quartz filters with a nominal pore size of ~1 µm. Samples for microbial sequencing were collected by pumping water directly onto sterilized 0.22 µm Sterivex polyvinylidene fluoride filters (EMD Millipore). Filters were frozen until shipped back to the University of Waterloo and subsequently kept at -80°C until processing.

Sediments were collected by freeze-coring[31] at 7 and 10 meters during the winter ice cover period at L227. The entire sediment profile was analyzed for $\delta^{13}C$ and $\delta^{15}N$ at 1 cm intervals. Selected samples were analyzed for $\delta^{56}Fe$. Additional sediment samples were also collected by subsampling an Eckman dredge at 1, 4, 8, and 10 meters in Lake 227 and at 1, 5 11, 13, 15, and 17 meters in Lake 442. The top 1 cm was collected from only those dredges where the surface was clearly visible and surface structures were undisturbed. Sediment traps constructed of acrylic tubes with a width to depth ratio of >8 were suspended at 2.0, 5.5, and 8.5 meters depth in the water column at 3 locations in the central part of L227. Samples for $\delta^{13}C$ of DIC and CH_4 were prepared by headspace equilibration after acidification. For analysis of $\delta^{15}N$ of NH_4^+, samples were prepared using a modified diffusion technique[32] with a precision of 0.3‰ in $\delta^{15}N$. Both $\delta^{13}C$ of DIC and CH_4 and $\delta^{15}N$ of NH_4^+ were then analyzed by GC-CF-IRMS using

an Agilent 6890 GC coupled to a Isochrom isotope ratio mass spectrometer (IRMS: Micromass
350 UK) with precision +/- 0.3‰. $\delta^{13}C$, $\delta^{15}N$, and C/N of POM on filters, freeze-dried DOM, lake sediments, sediment trap samples were analyzed by EA-CF-IRMS using a Carlo Erba Elemental Analyzer (CHNS-O EA1108) coupled with a Delta Plus (Thermo) isotope ratio mass spectrometer with a precision of 0.2‰ in $\delta^{13}C$ and 0.3‰ in $\delta^{15}N$.

Samples of POM, in water and sediment samples were analyzed for $\delta^{56}Fe$ of Fe by MC-
355 ICP-MS (Micromass Isoprobe) after purification using ion-exchange chromatography[33] and reported relative to the average of igneous rocks ($\delta^{56}Fe$ = 0.0±0.05‰) with a precision of 0.03‰ (2σ). Sediment samples were digested with concentrated HF and HNO_3 and then dried before loading onto the resin. The measured Fe isotope composition of the IRMM-019 Fe isotope standard was -0.08±0.05‰, which lies within error of the long-term value used in the lab of -
360 0.09‰ relative to average igneous rocks[33].

Microbial Community Analysis

Genomic DNA was extracted using the PowerWater Sterivex DNA Isolation Kit (MoBio) and quantified using agarose gel electrophoresis. The V3-V4 region of the bacterial 16S ribosomal RNA gene was amplified from each sample using triplicate PCR amplifications. Each
365 reaction contained ≤10 ng of sample DNA and used reagent, volumes, and thermocycler conditions described previously[34]. As an exception to this, modified forward and reverse primers 341f-808r were used for Illumina sequencing in a previously described configuration[35]. After combining triplicate reaction products, to reduce bias, products for each sample were pooled at a normalized concentration, gel purified using the Wizard SV Gel and PCR Clean-Up System
370 (Promega), and spiked with 8.5-10% PhiX prior to sequencing. Paired-end (2x250 bp) high-throughput DNA sequencing was carried out using the MiSeq platform (Illumina), achieving a

cluster density of 452-507 K/mm^2 with 92.9-98.0% of clusters passing filter. Raw demultiplexed sequencing reads were processed using the AXIOME software tool, version 1.5[36]. Using AXIOME, paired sequences were assembled using PANDAseq version 2.8[37], were chimera
375 checked and clustered at 97% using USEARCH version 7.0.1090[38], and were rarefied using QIIME version 1.9.0[39]. All sequences were deposited in [accession numbers to be inserted once sequence submission is complete].

To predict the major functional roles of the lake bacterial communities, the top ten most abundant bacterial OTUs within each water column sample, based on rarefied data, were
380 evaluated for their potential involvement in Fe or S oxidation or reduction, and methanotrophy. Representative sequences for each abundant OTU were assigned taxonomic ranks using the RDP Naïve Bayesian rRNA Classifier, version 2.10, with a confidence threshold of 50%, based on the RDP 16S rRNA training set 14[40,41]. If the classifier could not assign a rank at the genus level, OTU representative sequences were queried against the NCBI non-redundant nucleotide database
385 using BLASTN[42]. Cultured strains identified through the query with ≥97% sequence identity were used to assign, where possible, a single genus to the OTU. Subsequently, genera matched to each abundant OTU were checked against the literature for whether they contained strains with documented involvement in targeted metabolic activities. Any OTU classified within a genus that was found to contain a strain involved in one of these metabolic activities was inferred to have
390 the same potential metabolic activity. Potential metabolic functions of OTUs that could only be classified to the family level were inferred similarly. Any remaining OTUs were not assigned a metabolic role.

High abundance OTUs closely related to the photoferrotroph *C. ferrooxidans* were also examined phylogenetically to evaluate their placement within the green sulfur bacteria. Reference
395 16S rRNA gene sequences of cultured strains from the family *Chlorobiacaea*, along with an

appropriate outgroup sequence, were obtained from the Silva SSU-RefNR sequence database, release122[43]. Obtained sequences were aligned to representative sequences of each abundant *Chlorobium* OTU from L227 and L442 using SINA version 1.2.11[44], and the alignment was then truncated to the V3-V4 region of the 16S rRNA gene. Using this alignment, a phylogeny was
400 built using RAxML version 8.1.17[45], using 100 maximum likelihood searches and the GTRCAT sequence evolution model. Node support values were calculated using the Shimodaira-Hasegawa test. The resulting phylogeny was visualized using Dendroscope version 3.2.10[46].

References for Methods

28. Brunskill, G. J. & Schindler, D. W. Geography and bathymetry of selected lake basins, Experimental Lakes Area, northwestern Ontario. *J. Fish. Res. Bd. Can.* **28**, 139-155 (1971).

29. Stainton, M. P., Capel, M. & Armstrong, F. A. J. The chemical analysis of freshwater. 2nd Edition. *Can. Fish. Mar. Serv. Misc. Spec. Publ*. **25**: 166pp (1977).

30. Heyes, A. & Bell, J. T. Sulfide Analysis Using Ion Specific Electrode (With Preservation In Sulfide Anti-Oxidant Buffer) Appendix D, *Standard Operating Procedures*. Academy of Natural Sciences, St. Leonard, MD. (1999).

31. Crusius, J. & Anderson, R. F. Evaluating the mobility of ^{137}Cs, $^{239\,240}$Pu and ^{210}Pb from their distributions in laminated lake sediments. *J. Paleolimnol.* **13**, 119-141 (1995).

32. Spoelstra, J., Murray, M., & Elgood R. J. A simplified diffusion method for δ^{15}N analysis of dissolved ammonium. National Water Research Institute, Report Number 11-038. Environment Canada. 17 pp. (2011).

33. Beard, B. L. *et al*. Application of Fe isotopes to tracing the geochemical and biological cycling of Fe. *Chem. Geol*. **195**, (1-4), 87-117 (2003).

34. Kennedy, K., Hall, M. W., Lynch, M. D. J., Moreno-Hagelsieb, G. & Neufeld, J. D. Evaluating bias of Illumina-based bacterial 16S rRNA gene profiles. *Appl. Environ. Microbiol*. **80**, 5717–5722 (2014).

35. Bartram, A. K., Lynch, M. D., Stearns, J. C., Moreno-Hagelsieb, G. & Neufeld, J. D. Generation of multimillion-sequence 16S rRNA gene libraries from complex microbial communities by assembling paired-end Illumina reads. *Appl. Environ. Microbiol*. **77**, 3846–3852 (2011).

36. Lynch, M. D., Masella, A. P., Hall, M. W., Bartram, A. K. & Neufeld, J. D. AXIOME: automated exploration of microbial diversity. *GigaScience* **2**, 3 (2013).

37. Masella, A. P., Bartram, A. K., Truszkowski, J. M., Brown, D. G. & Neufeld, J. D. PANDAseq: paired-end assembler for Illumina sequences. *BMC Bioinformatics* **13**, 1–7 (2012).

38. Edgar, R. C. UPARSE: highly accurate OTU sequences from microbial amplicon reads. *Nat. Methods* **10**, 996–998 (2013).

39. Caporaso, J. G. *et al*. QIIME allows analysis of high-throughput community sequencing data. *Nat. Methods* **7**, 335-336 (2010).

40. Wang, Q., Garrity, G. M., Tiedje, J. M. & Cole, J. R. Naïve Bayesian classifier for rapid assignment of rRNA sequences into the new bacterial taxonomy. *Appl. Environ. Microbiol*. **73**, 5261-5267 (2007).

41. Cole, J. R. *et al*. Ribosomal Database Project: data and tools for high throughput rRNA analysis. *Nucleic Acids Res*. **42**, D633–D642 (2014).

42. Altschul, S. F., Gish, W., Miller, W., Myers, E. W. & Lipman, D. J. Basic local alignment
440 search tool. *J. Mol. Biol*. **215**, 403–410 (1990).

43. Quast, C. *et al*. The SILVA ribosomal RNA gene database project: improved data processing and web-based tools. *Nucleic Acids Res.* **41**, D590–D596 (2013).

44. Pruesse, E., Peplies, J. & Gloeckner, F. O. SINA: Accurate high-throughput multiple
445 sequence alignment of ribosomal RNA genes. *Bioinformatics* **28**, 1823–1829 (2012).

45. Stamatakis, A. RAxML version 8: a tool for phylogenetic analysis and post-analysis of large phylogenies. *Bioinformatics* **30**, 1312–1313 (2014).

450 46. Huson, D. H. & Scornavacca, C. Dendroscope 3: An interactive tool for rooted phylogenetic trees and networks. *Syst. Biol.* **61**, 1061–1067 (2012).

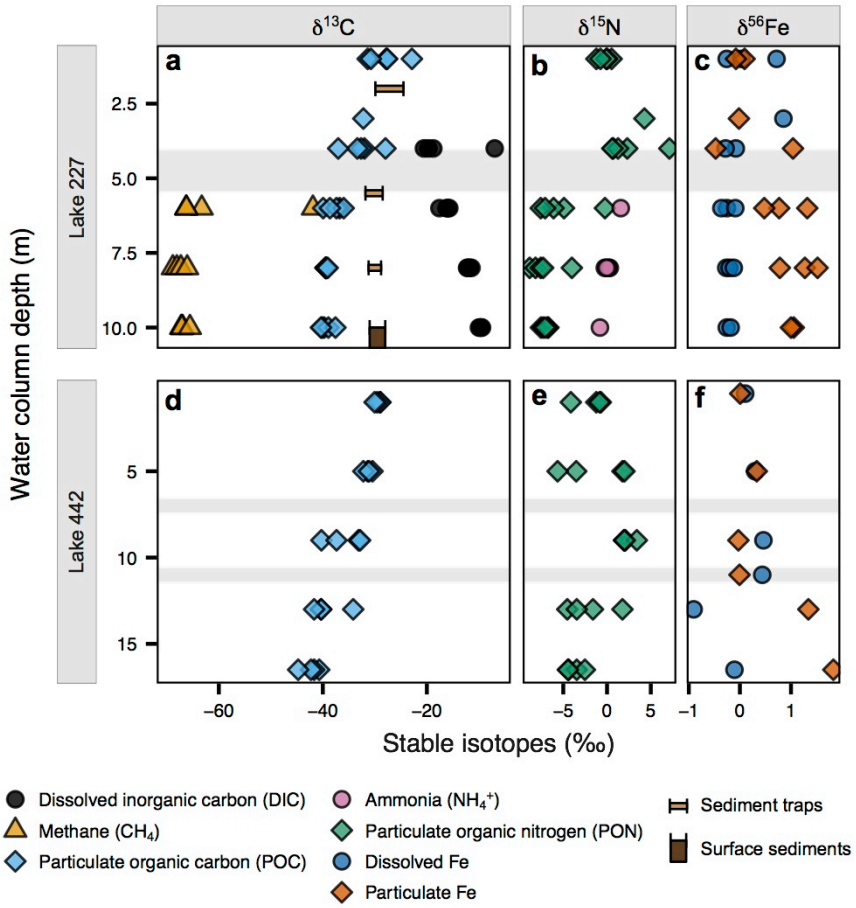

Figure 1 | Stable isotopic values in the water columns of (a-c) L227 and (d-f) L442. a, d, $\delta^{13}C$ in DIC, CH_4, and POC, sampled in June-August 2010 and July 2014. For $\delta^{13}C$ in sediment traps and surficial sediments (1-2 cm), the width of plotted sediment markers represents the range of $\delta^{13}C$ values measured across the summer of 2011. **b, e,** $\delta^{15}N$ in NH_4^+ and PON sampled in June-August 2010. **c, f,** $\delta^{56}Fe$ in dissolved and particulate Fe sampled in June-August 2011 and July 2014. In each L227 panel, the surface mixed layer is separated from the seasonally anoxic hypolimnion by a grey transition zone. Each panel for L442 is divided by grey transition zones into the surfaced mixed layer (top), the cool, oxic hypolimnion (middle), and the seasonally anoxic hypolimnion (bottom). The transition zones dividing each lake layer may vary seasonally and annually in both thickness and water column location (depth) due to differing climate.

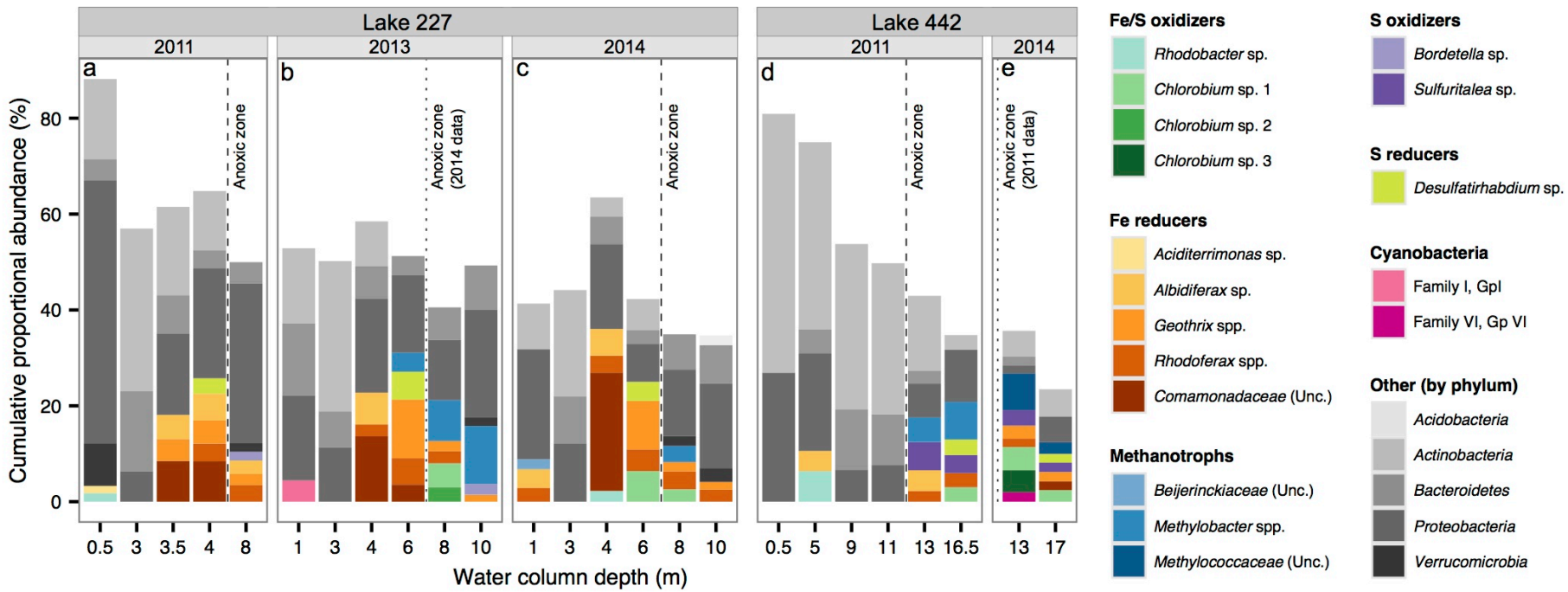

Figure 2 | Microbial community in the water columns of (a, b, c) L227 and (d, e) L442. In each depth sample, the ten most abundant bacterial operational taxonomic units (OTUs) are shown as stacked bars in terms of their proportional abundance within rarefied molecular sequencing data. Bacterial OTUs are grouped according to their potential involvement in Fe cycling, S cycling, and methanotrophy (see Methods). Cyanobacterial OTUs are also shown. For clarity, OTUs not associated with these metabolic roles are displayed at the phylum level. Potentially photoferrotrophic *Chlorobium* OTUs are shown with a naming and colour scheme matching that of Supplementary Data Fig. 2. Although not shown, *Chlorobium* sp. 1 is also present in the anoxic water column in L227 at 6 m depth in 2013 (rank 13, 2.9%) and in L442 at 13 m depth in 2011 (rank 31, 0.67%). All samples were collected between June 25th and July 9th in their respective sampling year.

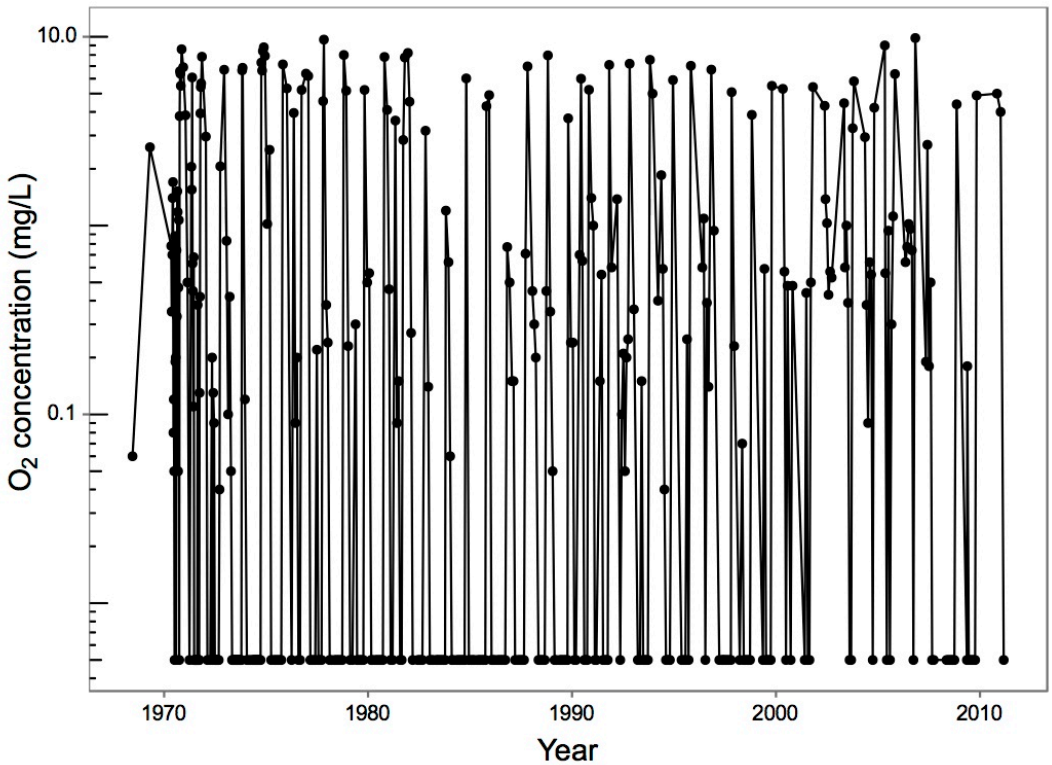

Figure 3 | Dissolved oxygen at 6 m depth in the L227 water column from 1969 to 2011. *Chlorobium* sequences were detected at high abundance at this depth in both 2013 and 2014 (Fig. 2). Dissolved oxygen samples were collected typically at least every two weeks in summer but
480 were collected at most twice during the winter. Following this sampling schedule, the full extent of the typical spring and fall re-oxygenation events (overturns) in L227 may not have been measured in some years. Dissolved oxygen is typically, but not always, measured after fall overturn. Spring overturn measurements can be missed following ice-off due to logistical reasons and especially in years when temperatures warm rapidly after ice-off. Thus, the oxygen record at
485 6 m reflects the minimum number of re-oxygenation events at this depth.

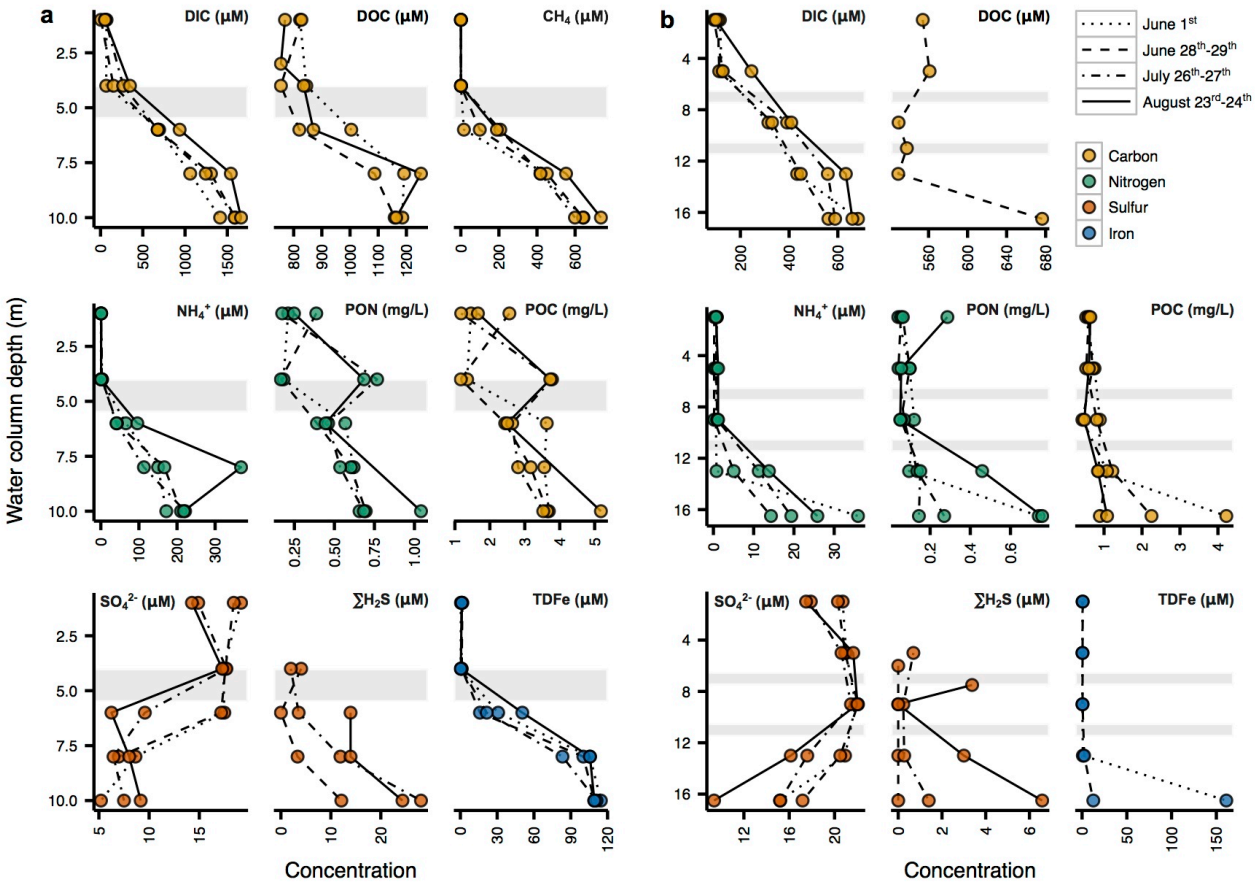

Supplementary Data Figure 1. Water chemistry of (a) L227 and (b) L442 water columns. All samples were collected in June-August 2010, and measurements from the same sampling dates are connected by lines for visual clarity. Sampling dates include those from before the onset of the annual cyanobacterial bloom (June 1st), during the bloom (June 28th-29th), and after the bloom (July 26th-27th, August 23rd-24th), in L227. In each sub-panel for L227, the surface mixed layer is separated from the seasonally anoxic hypolimnion by a grey transition zone. Each sub-panel for L442 is divided by grey transition zones into the surfaced mixed layer (top), the cool, oxic hypolimnion (middle), and the seasonally anoxic hypolimnion (bottom). The transition zones dividing each lake layer may vary seasonally and annually in both thickness and water column location (depth) due to differing climate.

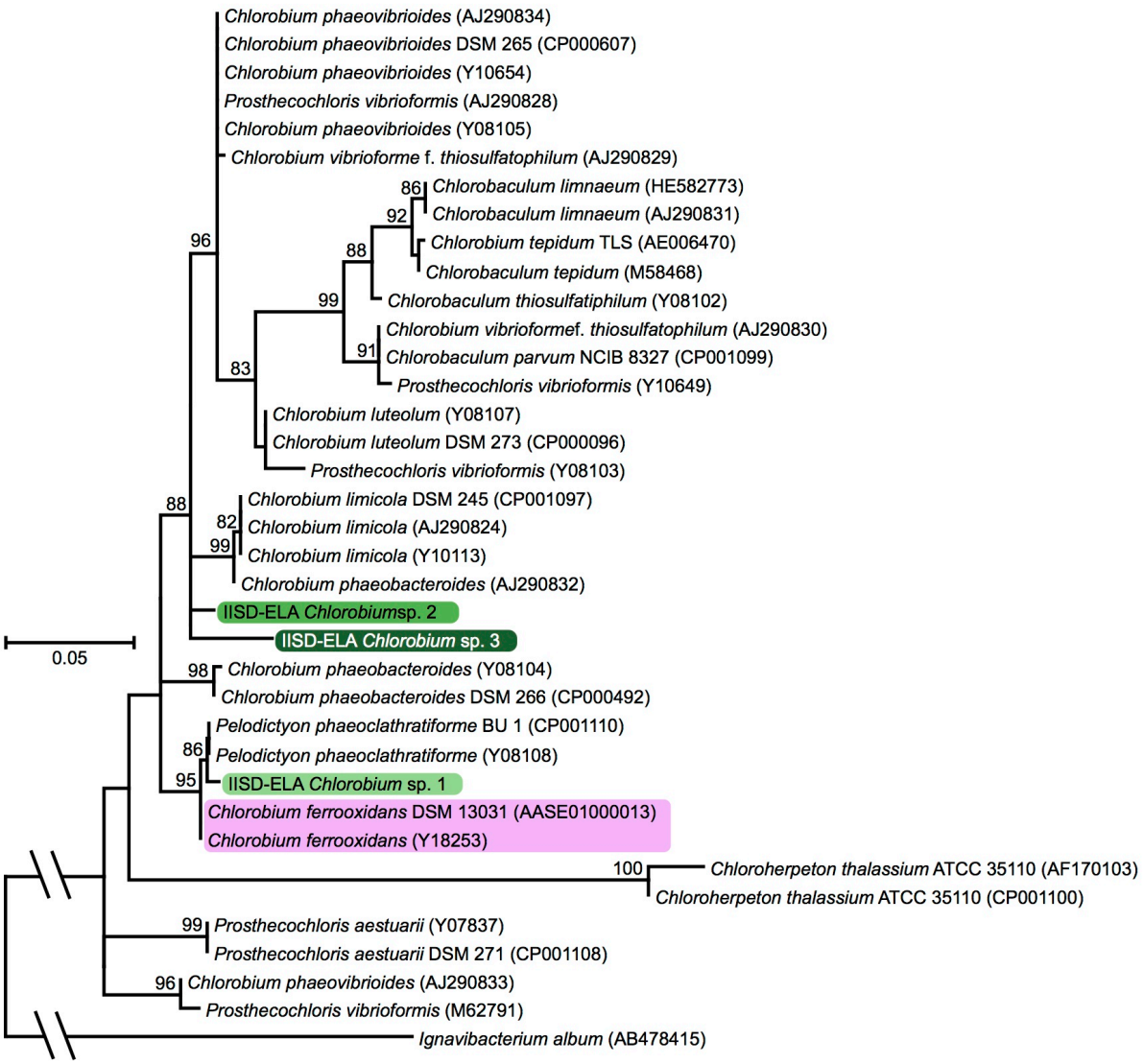

Supplementary Data Figure 2. Phylogenetic placement of potential photoferrotrophs within the family *Chlorobiaceae*. Reference *Chlorobiaceae* sequences represent cultured strains. Node support values, calculated using the Shimodaira-Hasegawa test, are shown where 80/100 or higher. Sequences highlighted in pink correspond to known photoferrotrophs, and those highlighted in green represent OTUs identified at high abundance in the water columns of L227 and L442 (Fig. 2). Importantly, IISD-ELA *Chlorobium* sp. 1 was identified at high abundance in the water columns of both lakes.

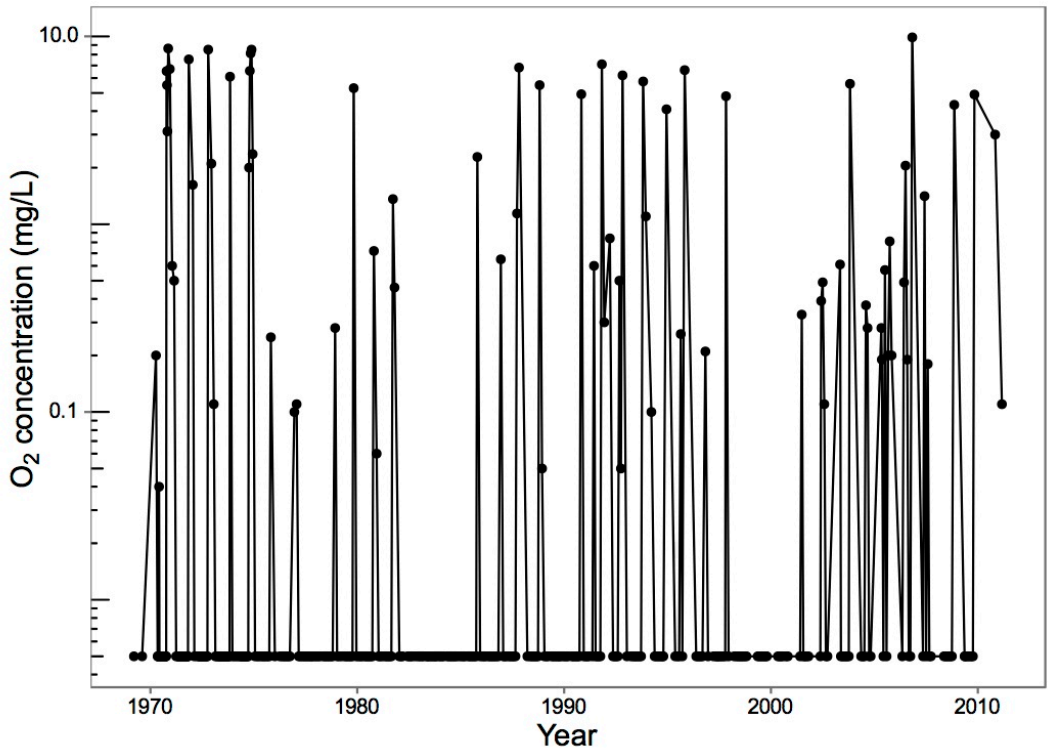

Supplementary Data Figure 3. Dissolved oxygen at 8 m depth in the L227 water column from 1969 to 2011. *Chlorobium* sequences were detected at high abundance in both 2013 and 2014 at this depth (Fig. 2). Dissolved oxygen samples were collected typically at least every two weeks in summer but were collected at most twice during the winter. Following this sampling schedule, the full extent of the typical spring and fall re-oxygenation events (overturns) in L227 may not have been measured in some years. Dissolved oxygen is typically, but not always, measured after fall overturn. Spring overturn measurements can be missed following ice-off due to logistic reasons and especially in years when temperatures warm rapidly after ice-off. Thus, the oxygen record at 8 m reflects the minimum number of re-oxygenation events at this depth.

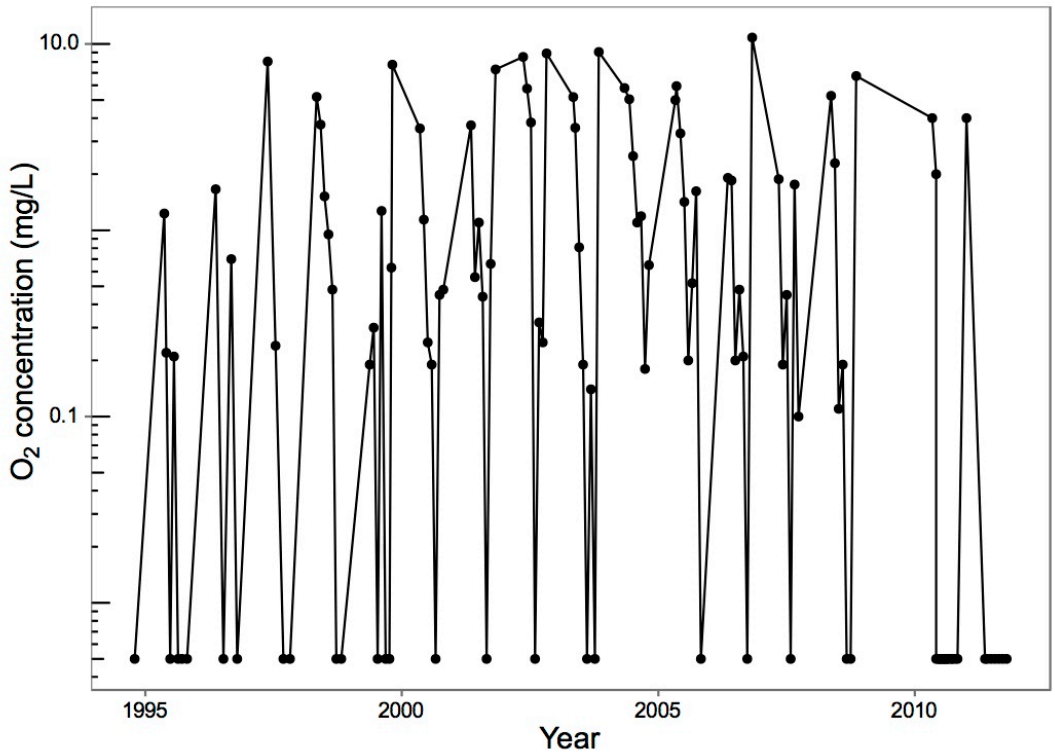

Supplementary Data Figure 4. Dissolved oxygen at 13 m depth in the L442 water column from 1994 to 2012. *Chlorobium* sequences were detected at high abundance at this depth in both 2011 and 2014 (Fig. 2). Dissolved oxygen samples were collected typically once per month in summer but were collected at most once during the winter. Following this sampling schedule, the full extent of the typical spring and fall re-oxygenation events (overturns) in L442 may not have been measured in some years. Dissolved oxygen is typically, but not always, measured after fall overturn. Spring overturn measurements can be missed following ice-off due to logistic reasons and especially in years when temperatures warm rapidly after ice-off. Thus, the oxygen record at 13 m reflects the minimum number of re-oxygenation events at this depth.